

The eccentricity distribution of compact binaries

I. Kowalska¹, T. Bulik^{1,2}, K. Belczynski^{1,3}, M. Dominik¹, and D. Gondek-Rosinska^{4,2}

¹ Astronomical Observatory, University of Warsaw, Al Ujazdowskie 4, 00-478 Warsaw, Poland

² Nicolaus Copernicus Astronomical Center, Bartycka 18, 00716, Warsaw, Poland

³ Dept. of Physics and Astronomy, University of Texas, Brownsville, TX 78520, USA

⁴ Institute of Astronomy, University of Zielona Góra, ul. Lubuska 2, 65-265 Zielona Góra, Poland

Received ; accepted

ABSTRACT

Context. The current gravitational wave detectors have reached their operational sensitivity and are nearing detection of compact object binaries. In the coming years, we expect that the Advanced LIGO/VIRGO will start taking data. At the same time, there are plans for third generation ground-based detectors such as the Einstein Telescope, and space detectors such as DECIGO.

Aims. We discuss the eccentricity distribution of inspiral compact object binaries during their inspiral phase. We analyze the expected distributions of eccentricities at three frequencies that are characteristic of three future detectors: Advanced LIGO/VIRGO (30 Hz), Einstein Telescope (3 Hz), and DECIGO (0.3 Hz).

Methods. We use the StarTrack binary population code to investigate the properties of the population of compact binaries in formation. We evolve their orbits until the point that they enter a given detector sensitivity window and analyze the eccentricity distribution at that time.

Results. We find that the eccentricities of BH-BH and BH-NS binaries are quite small when entering the Advanced LIGO/VIRGO detector window for all considered models of binary evolution. Even in the case of the DECIGO detector, the typical eccentricities of BH-BH binaries are below 10^{-4} , and the BH-NS eccentricities are smaller than 10^{-3} . Some fraction of NS-NS binaries may have significant eccentricities. Within the range of considered models, we found that a fraction of between 0.2% and 2% NS-NS binaries will have an eccentricity above 0.01 for the Advanced LIGO/VIRGO detectors. For the ET detector, this fraction is between 0.4% and 4%, and for the DECIGO detector it lies between 2% and 27%.

Key words. binaries – gravitational waves

1. Introduction

As the interferometric gravitational wave detectors LIGO and VIRGO (Harry & the LIGO Scientific Collaboration 2010; Acernese et al. 2006) reach their design sensitivities, the first detection of gravitational waves has become more imminent. Both detectors will undergo serious improvements to increase their sensitivity (Smith & LIGO Scientific Collaboration 2009; Spallicci et al. 2005).

It is therefore important to investigate the properties of the primary candidate sources for detection, namely compact object binaries. There have been a number of papers dealing with several properties of the population of compact binaries (e.g., Nelemans & van den Heuvel 2001; Voss & Tauris 2003; De Donder & Vanbeveren 2004; Sipior & Sigurdsson 2002; Pfahl et al. 2005; Dewi et al. 2002, 2005; Bogomazov et al. 2007; Kiel et al. 2010). In particular, Abadie et al. (2010) presented their estimated detection rates. In addition, the mass spectrum (Gondek-Rosińska et al. 2007), and even spin properties (Schnittman 2004; Mandel & O’Shaughnessy 2010) have been studied. In this paper, we present yet another aspect of the merging compact object binary population: the distribution of the eccentricity.

From radio observations, we currently know of only six compact object binaries with merger timescales shorter than a Hubble time, all of them NS-NS (neutron star - neutron star) systems, and we know of no BH-NS (black hole - neutron star) nor BH-BH (black hole - black hole) system. The known NS-NS systems are listed along with their orbital parameters in Table 1.

The observed NS-NS binaries have merger times $T_{\text{merg}} \gtrsim 100$ Myr. However, a significant fraction of the population of the merging NS-NS may originate in the so-called ultra-compact NS-NS binaries, which have much shorter merger timescales $T_{\text{merg}} \lesssim 100$ Myr (Belczynski et al. 2002a). In addition, the small number of known pulsars are indicative of there being a significant fraction of very eccentric binaries.

Since no BH-NS nor BH-BH binaries are known, we can only rely on evolutionary considerations when estimating their number and properties. It has been found that their number depends very strongly on the outcome of the common envelope phase when the secondary is on the Hertzsprung gap. This phase will very likely end up as a merger and the formation of a Thorne-Zytkow object. However, it has been demonstrated that in a low-metallicity environment the common envelope mergers may be (to some extent) avoided and the BH-BH formation is very effective (Belczynski et al. 2010b).

The eccentricity of a compact object binary may potentially be derived by analyzing the inspiral signal, provided that the eccentricity is significant. In this paper, we investigate the eccentricity distributions in the frequency band of the currently working and future detectors of gravitational waves. For the currently working detectors (LIGO and VIRGO), we assume that the sensitivity of the detectors will allow us to measure the signal for the frequencies starting at 30 Hz. This may not be accurate for the current state of these instruments, but it does accurately represent the predicted sensitivity of the Advanced LIGO/VIRGO detectors. We consider two future detectors: the Einstein Telescope (Van Den Broeck 2010) and DECIGO

(Kawamura 2006; Seto et al. 2001). For the Einstein Telescope, we assume that binaries shall be detectable from 3 Hz, and for DECIGO we assume that the lowest frequency detectable is 0.3 Hz. In all cases, these have to be treated as indicative numbers that roughly describe these instruments.

In section 2, we describe the model used to investigate the population of compact object binaries. Section 3 presents the results for the current and future gravitational wave detectors. In section 4, we summarize and discuss the results.

2. The model

2.1. Compact object binary population model

To model the population of compact object binaries, we used the StarTrack population synthesis code (Belczynski et al. 2002b). It performs a suite of Monte Carlo simulations of the stellar evolution of stars in environments of two typical metallicities: $Z = Z_{\odot} = 0.02$ and $Z = 10\% Z_{\odot} = 0.002$ (e.g., Belczynski et al. 2010b). In these calculations, we employed the recent estimates of mass loss rates (Belczynski et al. 2010a). We calculate a population of 2 million massive binary stars, tracking the ensuing formation of relativistic binary compact objects: double neutron stars (NS-NS), double black hole binaries (BH-BH), and mixed systems (BH-NS). Our modeling utilizes updated stellar and binary physics, including results from supernova simulations (Fryer & Kalogera 2001) and compact object formation (Timmes et al. 1996), incorporating elaborate mechanisms for treating stellar interactions such as mass transfer episodes (Belczynski et al. 2008) or tidal synchronization and circularization (Hut 1981). We place special emphasis on the common envelope evolution phase (Webbink 1984), which is crucial for close double compact object formation because the attendant mass transfer permits an efficient hardening of the binary. This orbital contraction can be sufficiently efficient to cause the individual stars in the binary to coalesce and form a single highly rotating object, thereby preventing additional binary evolution and the formation of a double compact object. Because of significant radial expansion, stars crossing the Hertzsprung gap (HG) very frequently initiate a common envelope phase. HG stars do not have a clear entropy jump at the core-envelope transition (Ivanova & Taam 2004); if such a star overflows its Roche lobe and initiates a common envelope phase, the inspiral is expected to lead to a coalescence (Taam & Sandquist 2000). In particular, it has been estimated that for a solar metallicity environment (e.g., our Galaxy), properly accounting for the HG gap may lead to a reduction in the merger rates of BH-BH binaries by $\sim 2 - 3$ orders of magnitude (Belczynski et al. 2007). In contrast, in a low metallicity environment this suppression is much less severe (~ 1 order of magnitude; Belczynski et al. (2010b)). The details of the common envelope phase are not yet fully understood, thus in what follows we consider two sets of models, one that does not take into account the suppression (optimistic models: marked with A), and another that assumes the maximum suppression (pessimistic models: marked with B). Solar metallicity and 10% of solar metallicity are labeled with Z and z, respectively. In the case of NSs, we adopt natal kick distributions from observations of single Galactic pulsars (Hobbs et al. 2005) with $\sigma = 265$ km/s. However, for BHs we draw kicks from the same distribution (but at a lower magnitude), which is inverse proportional to the amount of fall back expected at BH formation (e.g., Fryer & Kalogera 2001). In particular, for most massive BHs that form with the full fall back (direct BH formation), the amount of natal kick is zero. In addition, we test one more

set of models in which the magnitude of the NS kicks is lower by a factor of 2, to $\sigma = 132.5$ km/s, as some observations and empirically based arguments seem to indicate that natal kicks in close binaries are lower than for single stars (Dessart et al. 2006; Kitaura et al. 2006). The BH kicks are decreased in the similar fashion as in models with the full NS kicks. The standard value of σ parameter is denoted by K and the smaller value by k. The detailed list of models considered in this paper is presented in Table 2. Model AZK is a standard set of parameters described in detail by Belczynski et al. (2002b).

Table 2: The list of models of stellar evolution used in the paper.

Model	Metallicity	σ [kms ⁻¹]	HG
AZK	Z_{\odot}	265.0	+
BZK	Z_{\odot}	265.0	-
Azk	Z_{\odot}	132.5	+
Bzk	Z_{\odot}	132.5	-
AzK	10% Z_{\odot}	265.0	+
BzK	10% Z_{\odot}	265.0	-
Azk	10% Z_{\odot}	132.5	+
Bzk	10% Z_{\odot}	132.5	-

2.2. Evolution of orbits

The evolution of the orbit of compact object binary under the influence of gravitational radiation had been calculated by Peters & Mathews (1963); Peters (1964). In the quadrupole approximation, the orbit decays as

$$\frac{da}{dt} = -\frac{\beta}{a^3} \Psi(e), \quad \Psi(e) = \frac{1 + 73/24e^2 + 37/96e^4}{(1 - e^2)^{7/2}}, \quad (1)$$

where a is the great semi-axis, e is the eccentricity of binary, M_1 is the mass of the first component, M_2 is the mass of second component, and

$$\beta = \frac{64}{5} \frac{G^3 \mu M^2}{c^5}, \quad \mu = \frac{M_1 M_2}{M_1 + M_2}. \quad (2)$$

While the eccentricity decays as

$$\frac{de}{dt} = -\frac{19}{12} \frac{\beta}{a^4} \Phi(e), \quad \Phi(e) = \frac{(1 + 121/304e^2)e}{(1 - e^2)^{5/2}}. \quad (3)$$

Using the above formulae we can express the fundamental gravitational wave frequency as a function of the eccentricity

$$f_{GW}(e) = \frac{2}{P_0} \frac{(1 - e^2)^{3/2}}{e^{18/19}} \left[1 + \frac{121}{304} e^2 \right]^{-1305/2299} c_0^{3/2}, \quad (4)$$

where $c_0 = (e_0^{12/19} [1 + \frac{121}{304} e_0^2]^{1305/2299}) (1 - e_0^2)^{-1}$, P_0 is the initial orbital period, and $f_{GW}(e)$ is the first non-zero harmonic. The gravitational wave frequency is twice the orbital frequency, i.e., $f_{GW} = 2f_{orb} = \frac{2}{P_{orb}}$.

We present the evolution of eccentricity as a function of gravitational wave frequency in Figure 1 for a binary neutron star with components of equal masses of $1.4 M_{\odot}$. The initial frequency corresponds to a semi-major axis such that the merger time is set to be $T_{merg} = 10^4$ Myr. Figure 1 contains several different cases of evolution in the plane stretched by eccentricity and gravitational wave frequency.

Table 1: Known merging compact object binaries

Name	P_{orb} [h]	Present e	T_{merge} [Gyr]	e at 0.3 Hz	e at 3 Hz	e at 30 Hz	Ref.
J0737-3039A/B	2.454	0.088	0.085	4.5×10^{-5}	4×10^{-6}	3.5×10^{-7}	Burgay et al. (2003)
B2127+11C	8.05	0.681	0.2	2.9×10^{-4}	2.6×10^{-5}	2.3×10^{-6}	Anderson et al. (1990)
J1906+0746	3.98	0.085	0.3	2.6×10^{-5}	2.3×10^{-6}	2×10^{-7}	Lorimer et al. (2006)
B1913+16	7.752	0.617	0.3	2.2×10^{-4}	1.9×10^{-5}	1.7×10^{-6}	Weisberg & Taylor (2005)
J1756-2251	7.67	0.181	1.7	2.6×10^{-5}	2.5×10^{-6}	2.2×10^{-7}	Faulkner et al. (2005)
B1534+12 (=J1537+1155)	10.098	0.274	2.7	3.6×10^{-5}	3.2×10^{-6}	2.8×10^{-7}	Wolszczan (1991)

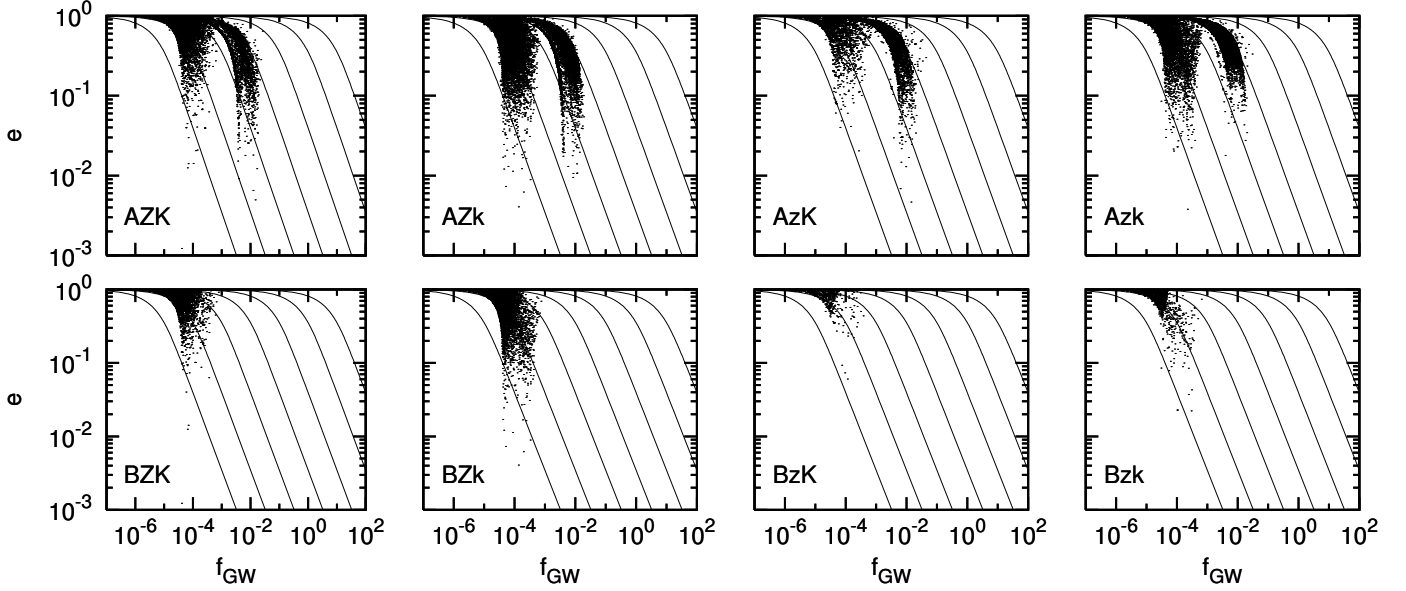


Fig. 2: The properties of the population of double neutron stars obtained using the StarTrack code. The plot shows only the binaries that will merge within the Hubble time. Solid lines correspond to evolutionary tracks for initial gravitational waves frequencies from $f_0 = 10^{-8}$ Hz (first line from the left-hand side) to $f_0 = 10^2$ Hz (first line from the right-hand side).

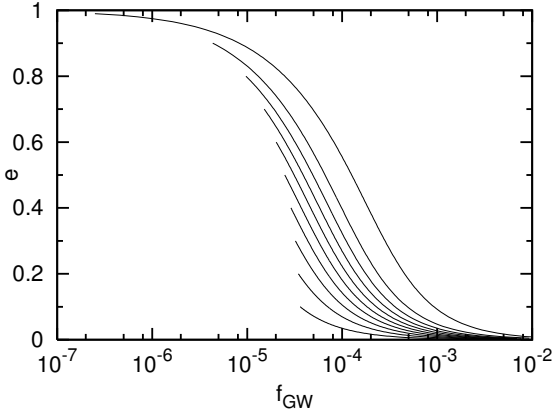


Fig. 1: We present ten cases of eccentricity evolution, starting with different values of e from $e = 0.1$ (first line from the bottom) to $e = 0.99$ (first line from the top). Initial semi-major axis is chosen such that a binary will merge within time $T_{merg} = 10$ Gyr in each case.

3. Results

3.1. Properties of the binaries at formation time

We start with an initial population created using the StarTrack code. We present the properties of the population of compact

object binaries in Figures 2 - 4 in the space spanned by the initial eccentricity and initial gravitational wave frequency, which is twice the orbital frequency. Each panel in these figures corresponds to a different model labeled as listed in Table 2.

The case of the NS-NS systems is shown in Figure 2. The boundary of the region populated by the systems on the left-hand side corresponds to the requirement that we only consider binaries that merge within a Hubble time. The bulk of the binaries shown in each panel correspond to those that have undergone one CE phase in their evolution. The top row corresponds to the models AZK, AZk, AzK, and Azk, in which we allow the binaries to cross through the common envelope with the donor on the Hertzsprung gap, denoted by "+" in Table 2. These binaries may undergo a second common envelope phase with a helium star companion. At the second CE stage, the orbit is tightened even more leading to formation of the stripe in the diagram stretching from $f_{GW} \approx 10^{-2}$ Hz at $e \approx 10^{-2}$. In these models, the initial distribution in the space of gravitational wave frequency versus eccentricity is bimodal. The influence of the value of the kick velocity has a small impact on the shape of distributions presented in Figure 2 as can be seen by comparing the data in plots labeled as either K-large kicks or k-small kicks.

For BH-NS systems, presented in Figure 3, and BH-BH binaries, in Figure 4, we present the results of six out of eight models, since in models BZK and BZk, almost no binaries are formed in our simulations that involve 2×10^6 initial binaries. For BH-NS and BH-BH binaries, the formation of ultra-compact binaries is not expected. The formation of NS-NS ultra-compact

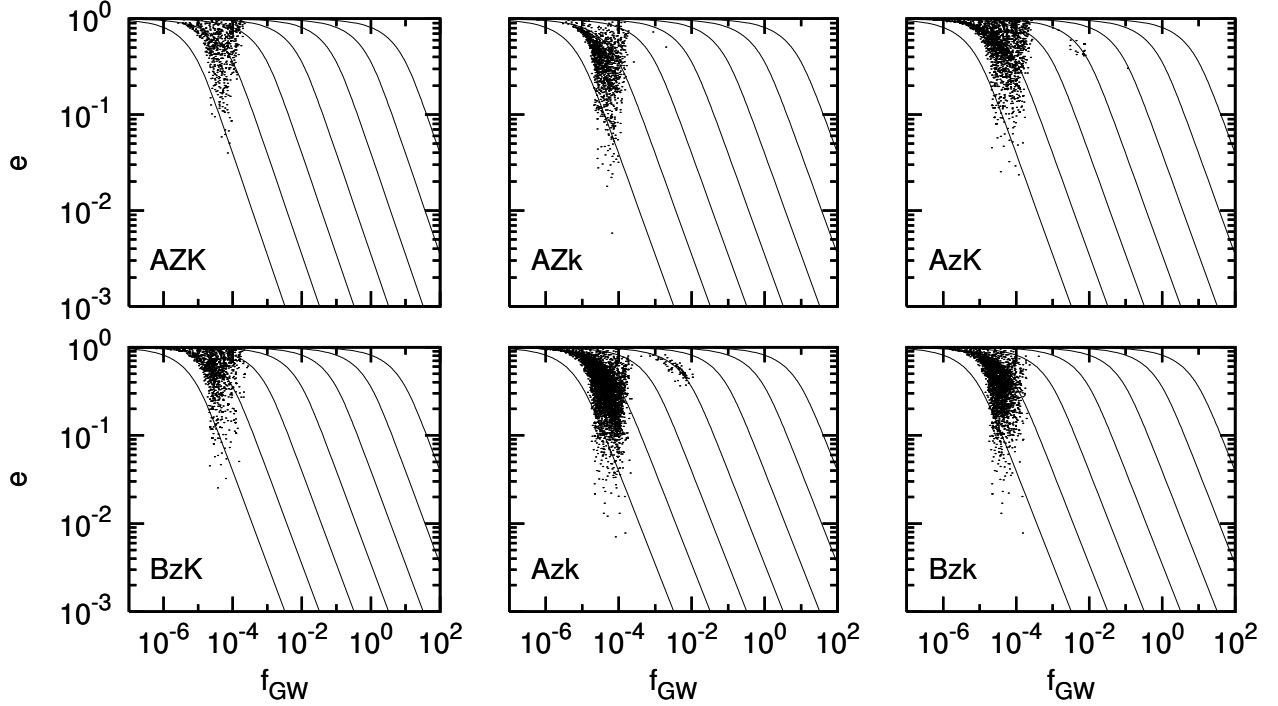


Fig. 3: The properties of the population of neutron star - black hole systems obtained using the StarTrack code. The plot shows only the binaries that will merge within the Hubble time. Solid lines correspond to evolutionary tracks for initial gravitational wave frequencies from $f_0 = 10^{-8}$ Hz (first line from the left-hand side) to $f_0 = 10^2$ Hz (first line from the right-hand side).

systems in very close orbits is the consequence of the final CE episode, which is initiated by a low-mass helium ($2-4 M_\odot$) star and its NS companion ($1.4 M_\odot$). Since the donor is about twice as massive as its companion, the CE phase is initiated by the non-stable mass transfer and the orbit significantly decreased in size. For more massive BH-BH/BH-NS binaries, helium stars are on average more massive ($M > 3-4 M_\odot$) and do not expand (so no CE phase), and even if a low mass helium star forms, then its companion is a BH ($M > 3 M_\odot$), so most likely instead of CE the RLOF is stable and does not lead to orbital decay (mass ratio ~ 1). Very few systems (e.g., models AzK or Azk) produce ultra-compact BH-NS/BH-BH binaries for very special cases of binary evolution. In the case of BH-BH binaries, shown in Figure 4 we present only six models, since models BZK and BZk do not lead to the formation of BH-BH binaries (Belczynski et al. 2007). In all models, there is an enhanced density of systems formed with $e \approx 0.1$ at approximately $10^{-5} \text{ Hz} < f_{\text{GW}} < 10^{-4} \text{ Hz}$. In these systems, the second black hole has formed via direct collapse. When treating the direct collapse, we assume that 10% of the mass escapes in the form of neutrinos and possibly gravitational waves. Hence, the gravitational mass of the BH is 10% lower than the baryon mass of the collapsing star. This introduces a small eccentricity ≈ 0.1 since the systems were circularized in the mass transfer prior to the collapse and the formation of the second BH.

3.2. Eccentricity when binary enters detector band

For the detection of gravitational waves, it is important to know the eccentricity of a binary at the time it enters the sensitivity window of the detector. We consider three cases that correspond approximately to three types of detectors. In Figure 5, we show the eccentricity distributions at 0.3 Hz (bottom horizontal axis)

and 3 Hz (top horizontal axis) corresponding approximately to the ET and DECIGO detectors. The results for the Advanced LIGO/VIRGO can be easily obtained by rescaling the horizontal axis.

The shape of the eccentricity distributions at the moment that the binary enters the given detector band follows from the corresponding initial distribution. However, one must note that for each type of binary there is a different natural timescale and frequency, because of the different mass scales of each binary.

We present the results for the DECIGO detector and add appropriate numbers for the ET in parentheses. For the NS-NS binaries shown in the top panel of Figure 5, the distribution is either centered on $e \approx 10^{-4}$ (ET: 10^{-5}) for the models BZK, BZk, BzK, and Bzk, where we do not allow the formation of ultra-compact binaries in a second CE phase. The remaining models AZK, AZk, AzK, and Azk contain another component centered roughly at $e \approx 10^{-4}$ (ET: 10^{-3}). This additional component represent the ultra-compact binaries that have experienced two episodes of mass transfer in their evolutionary history and were already very tight at the second supernova explosion. The mixed BH-NS binaries, shown in the middle panel of Figure 5 exhibit a distribution of eccentricity centered at $e \approx 3 \times 10^{-5}$ (ET: 3×10^{-6}), while the eccentricity BH-BH binaries, shown in the bottom panel of Figure 5 lie between $e \approx \times 10^{-6}$ (ET: 10^{-7}) and $e \approx \times 10^{-4}$ (ET: 10^{-5}).

For the Advanced LIGO/VIRGO detectors where we assume that the low frequency boundary lies at ≈ 30 Hz, the eccentricities are even smaller. It follows from equation 4 that the distributions are shifted by a factor of $10^{-19/18}$ for each factor of ten in frequency. Thus, the values of eccentricity in the case of Advanced LIGO/VIRGO type detectors are consistent with $e = 0$ and we can safely assume that all BH-NS and BH-BH binaries are circular without any loss of sensitivity.

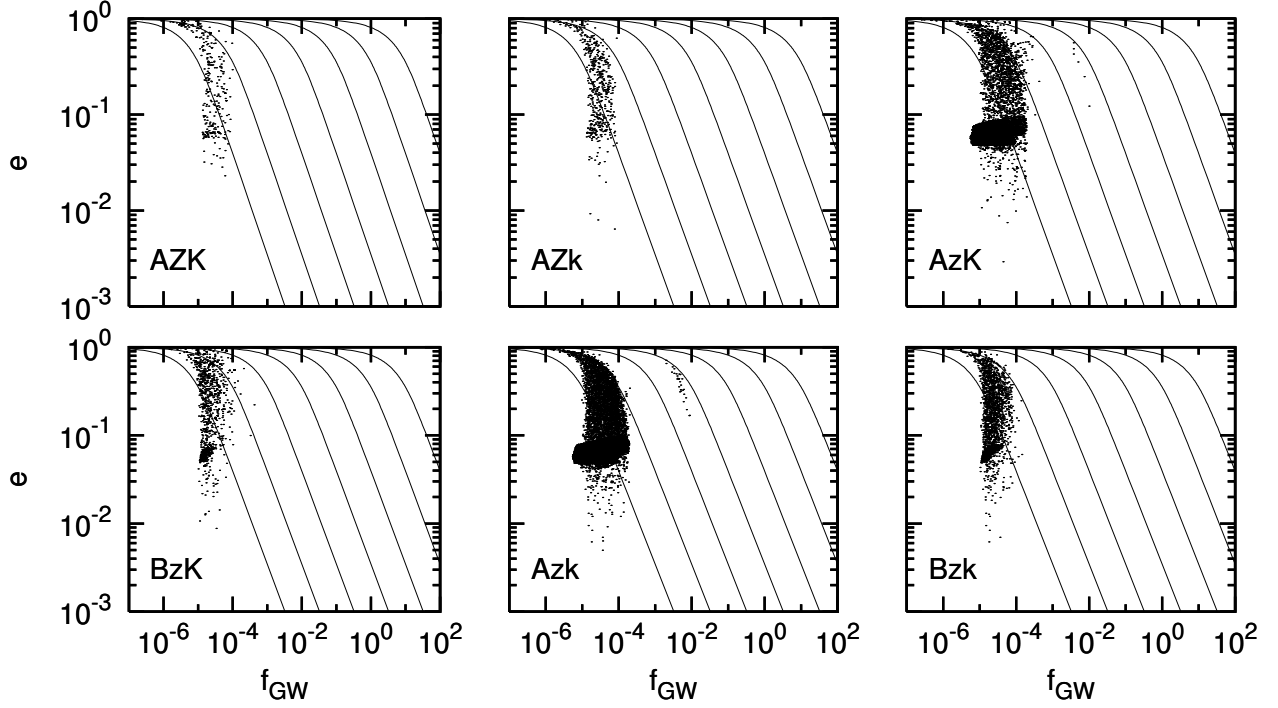


Fig. 4: The properties of the population of double black holes obtained using the StarTrack code. The plot shows only the binaries that will merge within the Hubble time. Solid lines correspond to evolutionary tracks for initial gravitational waves frequencies from $f_0 = 10^{-8}$ Hz (first line from the left-hand side) to $f_0 = 10^2$ Hz (first line from the right-hand side).

In table 3, we present the fraction of binaries with eccentricities above 0.01 at the time of entering the detector band, to help quantify the extent of the large eccentricity tails of the distributions presented in Figure 5. This fraction does not reflect the detectability of eccentricity (Shapiro Key & Cornish 2010), which for realistic distributions of binaries will be discussed in a forthcoming paper.

4. Summary

We have presented the eccentricity distributions of compact object binaries at three frequencies immediately before merger. The properties of the compact object binaries have been calculated using the StarTrack population synthesis code. We have found that the eccentricity distributions of the compact object binaries do not depend strongly on the assumed model of binary evolution. Any dependence has been found to be the strongest for binary neutron stars, whose distributions may be either single or double peaked. The extra peak corresponds to ultra-compact NS-NS binaries that have undergone an additional CE phase immediately before forming the second NS.

To make the results easier to use in the simulations, we have fitted the resulting distributions of eccentricity with a single log-normal distribution in the case of BH-BH and BH-NS binaries

$$f(x) = \frac{1}{\sigma\sqrt{2\pi}} \exp\left(-\frac{(x-\mu)^2}{2\sigma^2}\right), \quad (5)$$

where $x = \log e$, μ is the mean, and σ is the variance.

For the NS-NS eccentricities, we used a sum of two log-normal distributions with two weights, since the distribution is double peaked, given by

$$f(x) = \frac{w}{\sigma_1\sqrt{2\pi}} \exp\left(-\frac{(x-\mu_1)^2}{2\sigma_1^2}\right) + \frac{(1-w)}{\sigma_2\sqrt{2\pi}} \exp\left(-\frac{(x-\mu_2)^2}{2\sigma_2^2}\right) \quad (6)$$

Table 3: Fraction of the compact binaries with eccentricity greater than 10^{-2} . Top table corresponds to double neutron stars (NS-NS), middle to the mixed systems (BH-NS), and the bottom to the binary black holes (BH-BH). We present the fraction of binaries at the moment of entering different frequency bands (30 Hz, 3 Hz, and 0.3 Hz). In brackets, we include the number of these systems in the simulation N . We only listed results for models that are non-zero. The number of digits shown is for formatting only, and the relative sampling error is $N^{-1/2}$.

NS-NS					
	30 Hz		3 Hz		0.3 Hz
AZK	0.60% (51)	1.32%	(112)	11.13%	(945)
BZK	1.27% (36)	2.33%	(66)	6.52%	(185)
AZk	0.16% (27)	0.38%	(64)	10.37%	(1732)
BZk	0.30% (15)	0.75%	(37)	2.22%	(110)
AzK	0.29% (25)	0.96%	(83)	21.74%	(1880)
BzK	1.87% (13)	4.02%	(28)	9.33%	(65)
Azk	0.26% (37)	0.57%	(81)	26.91%	(3799)
Bzk	1.74% (21)	3.31%	(40)	7.79%	(94)
BH-NS					
	30 Hz		3 Hz		0.3 Hz
AZK	0.29% (2)	0.73%	(5)	3.05%	(21)
AZk	0.15% (2)	0.54%	(7)	0.61%	(8)
AzK	0.56% (14)	0.96%	(24)	3.96%	(99)
BzK	0.68% (10)	1.23%	(18)	3.63%	(53)
Azk	0.35% (15)	0.78%	(34)	2.81%	(122)
Bzk	0.33% (8)	0.91%	(22)	1.53%	(37)
BH-BH					
	30 Hz		3 Hz		0.3 Hz
AZK	0.31% (1)	0.62%	(2)	1.87%	(6)
AzK	0.02% (3)	0.02%	(4)	0.13%	(23)
BzK	0.15% (2)	0.15%	(2)	0.46%	(6)
Azk	0.00% (1)	0.01%	(2)	0.03%	(6)

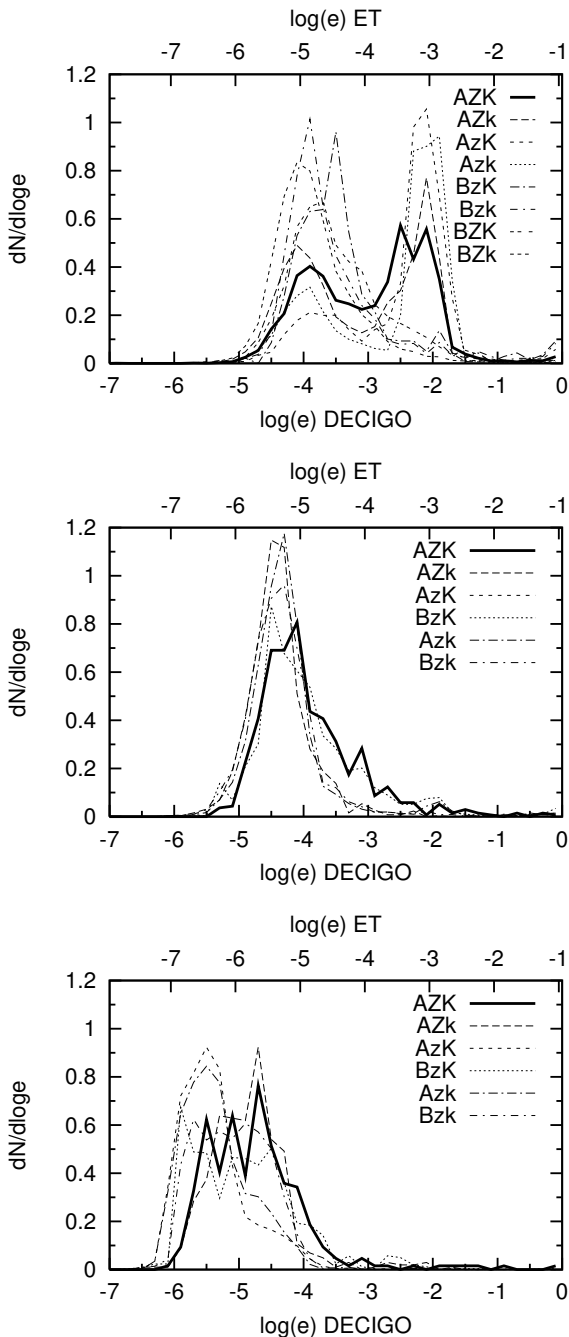


Fig. 5: Distribution of eccentricity for (NS-NS - top panel, BH-NS middle panel and BH-BH bottom panel) seen at 0.3 Hz (DECIGO-like detectors) and at 3 Hz (ET-like detectors). Solid thick line corresponds to standard model (AZK). Dashed and dotted lines indicate other models.

where $x = \log e$, μ_1 is the mean of the first peak, μ_2 is the mean of the second peak, σ_1 is the variance of the first distribution, σ_2 is the variance of the second distribution, and w is the weight.

We used the Marquardt-Levenberg algorithm to find the parameters, and estimate the asymptotic standard error of each of them. The results of the fits are shown in Table 4. The widths of the distributions σ are the same for each frequency band and only the centroids move.

The eccentricity of the BH-BH binaries in all three cases is negligible. This is due to two factors. First, at the frequencies of interest the BH-BH systems are much closer to coalescence than

Table 4: Parameters of log normal distribution fitted to results of model AZK with asymptotic standard errors.

NS-NS			
σ_1 :	0.47 ± 0.04		
σ_2 :	0.39 ± 0.03		
w :	0.46 ± 0.03		
	0.3 Hz	3 Hz	30 Hz
μ_1	-3.83 ± 0.04	-4.89 ± 0.04	-5.94 ± 0.04
μ_2	-2.32 ± 0.03	-3.38 ± 0.03	-4.43 ± 0.03
BH-NS			
σ :	0.55 ± 0.03		
	0.3 Hz	3 Hz	30 Hz
μ	-4.18 ± 0.04	-5.23 ± 0.03	-6.27 ± 0.03
BH-BH			
σ :	0.70 ± 0.03		
	0.3 Hz	3 Hz	30 Hz
μ	-4.91 ± 0.08	-5.95 ± 0.03	-7.06 ± 0.03

the neutron star. Second, the initial kicks at formation of BHs are lower than in the case of NS, so the initial eccentricities of BH-BH systems are typically lower than in the case of NS-NS ones.

The eccentricities of the mixed BH-NS systems are larger than in the case of BH-BH ones. However, the number of systems is small enough to ensure that by neglecting the eccentricity we do not decrease the sensitivity of Advanced LIGO/VIRGO detectors. For the ET-like detector, some eccentric systems may be detected. In the case of the DECIGO-like detector, the number of systems with eccentricities above 0.01 lies between 3% and 4%.

The eccentricity of NS-NS systems are larger than those of binaries containing BHs. Given a much larger expected detection rate for ET, this means that there should be a significant number of NS-NS binaries with detectable eccentricities. Finally, in the case of DECIGO a fraction of between 2% and 27% of the NS-NS binaries have eccentricities above 0.01. Moreover, the shape of the eccentricity distribution of NS-NS binaries will depend on the existence of an evolutionary scenario leading to the formation of ultra-compact binaries. Thus, the measurement of the eccentricity distribution is an interesting tool for probing the details of NS-NS formation scenarios.

Acknowledgments

This work was supported by the EGO-DIR-102-2007; the FOCUS 4/2007 Program of Foundation for Polish Science, the Polish grants N N203 511238, DPN/N176/VIRGO/2009, N N203 302835, N N203 404939 and by CompStar a Research Networking Programme of the European Science Foundation.

References

- Abadie, J., Abbott, B. P., Abbott, R., et al. 2010, *Classical and Quantum Gravity*, 27, 173001
- Acernese, F., Amico, P., Al-Shourbagy, M., et al. 2006, *Classical and Quantum Gravity*, 23, 63
- Anderson, S. B., Gorham, P. W., Kulkarni, S. R., Prince, T. A., & Wolszczan, A. 1990, *Nature*, 346, 42
- Belczynski, K., Bulik, T., Fryer, C. L., et al. 2010a, *ApJ*, 714, 1217
- Belczynski, K., Bulik, T., & Kalogera, V. 2002a, *ApJ*, 571, L147
- Belczynski, K., Dominik, M., Bulik, T., et al. 2010b, *ApJ*, 715, L138
- Belczynski, K., Kalogera, V., & Bulik, T. 2002b, *ApJ*, 572, 407
- Belczynski, K., Kalogera, V., Rasio, F. A., et al. 2008, *ApJS*, 174, 223

- Belczynski, K., Taam, R. E., Kalogera, V., Rasio, F. A., & Bulik, T. 2007, *ApJ*, 662, 504
- Bogomazov, A. I., Lipunov, V. M., & Tutukov, A. V. 2007, *Astronomy Reports*, 51, 308
- Burgay, M., D’Amico, N., Possenti, A., et al. 2003, *Nature*, 426, 531
- De Donder, E. & Vanbeveren, D. 2004, *New A*, 9, 1
- Dessart, L., Burrows, A., Ott, C. D., et al. 2006, *ApJ*, 644, 1063
- Dewi, J. D. M., Podsiadlowski, P., & Pols, O. R. 2005, *MNRAS*, 363, L71
- Dewi, J. D. M., Pols, O. R., Savonije, G. J., & van den Heuvel, E. P. J. 2002, *MNRAS*, 331, 1027
- Faulkner, A. J., Kramer, M., Lyne, A. G., et al. 2005, *ApJ*, 618, L119
- Fryer, C. L. & Kalogera, V. 2001, *ApJ*, 554, 548
- Gondek-Rosińska, D., Bulik, T., & Belczyński, K. 2007, *Advances in Space Research*, 39, 285
- Harry, G. M. & the LIGO Scientific Collaboration. 2010, *Classical and Quantum Gravity*, 27, 084006
- Hobbs, G., Lorimer, D. R., Lyne, A. G., & Kramer, M. 2005, *MNRAS*, 360, 974
- Hut, P. 1981, *A&A*, 99, 126
- Ivanova, N. & Taam, R. E. 2004, *ApJ*, 601, 1058
- Kawamura, S. 2006, *Astronomical Herald*, 99, 490
- Kiel, P. D., Hurley, J. R., & Bailes, M. 2010, *MNRAS*, 406, 656
- Kitaura, F. S., Janka, H., & Hillebrandt, W. 2006, *A&A*, 450, 345
- Lorimer, D. R., Stairs, I. H., Freire, P. C., et al. 2006, *ApJ*, 640, 428
- Mandel, I. & O’Shaughnessy, R. 2010, *Classical and Quantum Gravity*, 27, 114007
- Nelemans, G. & van den Heuvel, E. P. J. 2001, *A&A*, 376, 950
- Peters, P. C. 1964, *Physical Review*, 136, 1224
- Peters, P. C. & Mathews, J. 1963, *Physical Review*, 131, 435
- Pfahl, E., Podsiadlowski, P., & Rappaport, S. 2005, *ApJ*, 628, 343
- Schnittman, J. D. 2004, *Phys. Rev. D*, 70, 124020
- Seto, N., Kawamura, S., & Nakamura, T. 2001, *Physical Review Letters*, 87, 221103
- Shapiro Key, J. & Cornish, N. J. 2010, *ArXiv e-prints*
- Sipior, M. S. & Sigurdsson, S. 2002, *ApJ*, 572, 962
- Smith, J. R. & LIGO Scientific Collaboration. 2009, *Classical and Quantum Gravity*, 26, 114013
- Spallicci, A. D. A. M., Aoudia, S., de Freitas Pacheco, J., Regimbau, T., & Frossati, G. 2005, *Classical and Quantum Gravity*, 22, 461
- Taam, R. E. & Sandquist, E. L. 2000, *ARA&A*, 38, 113
- Timmes, F. X., Woosley, S. E., & Weaver, T. A. 1996, *ApJ*, 457, 834
- Van Den Broeck, C. 2010, *ArXiv e-prints*
- Voss, R. & Tauris, T. M. 2003, *MNRAS*, 342, 1169
- Webbink, R. F. 1984, *ApJ*, 277, 355
- Weisberg, J. M. & Taylor, J. H. 2005, in *Astronomical Society of the Pacific Conference Series*, Vol. 328, *Binary Radio Pulsars*, ed. F. A. Rasio & I. H. Stairs, 25–+
- Wolszczan, A. 1991, *Nature*, 350, 688